The Crystal Structure of the Platelet Activator Aggretin Reveals a Novel $(\alpha\beta)_2$ Dimeric Structure[†,‡]

Elizabeth Hooley,[§] Evangelos Papagrigoriou,[§] Alexei Navdaev,[||,⊥] Amit V. Pandey,[||,@] Jeannine M. Clemetson,[||] Kenneth J. Clemetson,[||] and Jonas Emsley*[,§]

Centre for Biomolecular Sciences, School of Pharmacy, University of Nottingham, Nottingham NG7 2RD, U.K., and Theodor Kocher Institute, University of Berne, Freiestrasse 1, CH-3012 Berne, Switzerland

Received March 27, 2008; Revised Manuscript Received June 3, 2008

ABSTRACT: Aggretin is a C-type lectin purified from *Calloselasma rhodostoma* snake venom. It is a potent activator of platelets, resulting in a collagen-like response by binding and clustering platelet receptor CLEC-2. We present here the crystal structure of aggretin at 1.7 Å which reveals a unique tetrameric quaternary structure. The two $\alpha\beta$ heterodimers are arranged through 2-fold rotational symmetry, resulting in an antiparallel side-by-side arrangement. Aggretin thus presents two ligand binding sites on one surface and can therefore cluster ligands in a manner reminiscent of convulxin and flavocetin. To examine the molecular basis of the interaction with CLEC-2, we used a molecular modeling approach of docking the aggretin $\alpha\beta$ structure with the CLEC-2 N-terminal domain (CLEC-2N). This model positions the CLEC-2N structure face down in the "saddle"-shaped binding site which lies between the aggretin α and β lectin-like domains. A 2-fold rotation of this complex to generate the aggretin tetramer reveals dimer contacts for CLEC-2N which bring the N- and C-termini into the proximity of each other, and a series of contacts involving two interlocking β-strands close to the N-terminus are described. A comparison with homologous lectin-like domains from the immunoreceptor family reveals a similar but not identical dimerization mode, suggesting this structure may represent the clustered form of CLEC-2 capable of signaling across the platelet membrane.

The first steps of platelet activation are critical to our understanding of hemostasis and thrombosis (*1*). Exposed matrix components from the subendothelium at sites of vascular damage interact with specific receptors on the surface of platelets, causing platelet activation and spreading to cover the injured site until it has regenerated. Snake venom proteins have been shown to bind a number of platelet receptors involved in platelet function (*1–3*). In many cases, they bind specifically to platelet surface glycoprotein receptors and either block function or activate and thus induce platelet activation via clustering of receptors. Hence, they are frequently used to study mechanisms of platelet activation and aggregation and belong to two major protein families, the C-type lectin family and the metalloproteinase disintegrin cysteine-rich protein family (*4*).

Crystal structures of the snake venom C-type lectins reveal these are $\alpha\beta$ heterodimers (*5–10*). The dimers are formed by a domain-swapping long loop, which leads to the disruption of the carbohydrate binding site and therefore loss of lectin activity. Aggretin, also known as rhodocytin, has been shown to bind to platelets (*11, 12*), causing a collagen-like response, which is characterized by a distinct lag phase before initiation of a signaling cascade involving activation of Syk and PLCγ2 leading to platelet aggregation (*11–14*). This signaling response is also similar to that seen in the autosomal recessive disorder Chediak-Higashi syndrome (CHS) (which is a granule release defect) (*15*). Aggretin has been shown to bind CLEC-2,[1] GPIbα, and integrin $\alpha2\beta1$; however, knockout studies have disputed a role for the latter two receptors in aggretin activity. Navdaev et al. (*14*) used antibodies against the thrombin binding site of GPIbα to inhibit the aggretin response in platelets. Chung et al. (*16*) used the GPIbα agonist agkistin to inhibit the aggretin response, whereas Bergmeier et al. (*17*) and Shin and Morita (*12*) showed that platelets without the 45 kDa N-terminal domain of GPIbα respond to aggretin and that echicetin did not inhibit the aggretin response. Navdaev et al. (*14*) and Chung et al. (*16*) also used antibodies against $\alpha2\beta1$ to inhibit the aggretin response. Suzuki-Inoue et al. (*18*) showed that aggretin-Sepharose bound $\alpha2\beta1$-loaded liposomes. Eble et

[†] E.H. is funded by the British Heart Foundation. K.J.C. thanks the Swiss National Science Foundation for support by Grants 31-063868.00 and 31-107754.04.

[‡] Coordinates and structure factors have been submitted to the Protein Data Bank (PDB) as entry 3BX4.

* To whom correspondence should be addressed. E-mail: jonas.emsley@nottingham.ac.uk. Telephone: +44 1158467092. Fax: +44 1158468002.

[§] University of Nottingham.

[||] University of Berne.

[⊥] Current address: Institute for Physiological Chemistry, Muenster Hospital, D-48149 Muenster, Germany.

[@] Current address: Department Klinische Forschung, Tiefenaulabors-DKF-Spital Bern, University of Berne, Tiefenaulabors 120, CH-3004 Berne, Switzerland.

[1] Abbreviations: CLEC-2, C-type lectin-like receptor 2; GpIb, platelet glycoprotein Ib; NKG2D, natural killer cell receptor G2D; HIV, human immunodeficiency virus.

10.1021/bi800528t CCC: $40.75
Published on Web 07/03/2008

al., (*19*) however, showed that aggretin did not bind to recombinant α2β1.

CLEC-2 is a type II transmembrane receptor found on platelets, monocytes, dendritic cells, and granulocytes and in the liver (*20*). The interaction with aggretin has been characterized in some biochemical detail, and mutagenesis of the recombinant CLEC-2 N-terminal domain revealed that the long loop region contained residues important for aggretin binding (*21*). The physiological ligand for CLEC-2 has not yet been identified, although pathological ligands include HIV-1 and podoplanin (*22–24*). Podoplanin is a transmembrane sialoglycoprotein found on various cancer cells, including squamous cell carcinomas (*25*), brain tumors (*26*), and testicular seminoma (*27*). Tumor-cell induced platelet aggregation by podoplanin is also involved in metastasis and lymphatic vessel formation. The interaction of podoplanin with CLEC-2 is dependent on the O-linked sialic acid groups on Thr52 (*28*). The interaction between podoplanin and CLEC-2 causes the same response in platelets as aggretin−CLEC-2 binding, indicating possible similarities in binding mode. Here we report the high-resolution structure of aggretin and show that it has a novel quaternary structure not previously seen in C-type lectin-like snake venom proteins. Modeling studies support a mechanism in which aggretin dimerizes CLEC-2 and activates platelets through a receptor clustering mechanism.

EXPERIMENTAL PROCEDURES

Crystallization. Aggretin was purified from *Calloselasma rhodostoma* crude snake venom by gel filtration and ion exchange chromatography as previously described (*14*). The purified protein was concentrated to 12 mg/mL in 50 mM ammonium acetate buffer (pH 5.0). Crystals were grown by the sitting drop vapor diffusion method at 20 °C in 2.4 M ammonium sulfate, 25 mM ammonium acetate (pH 5.0), and 2% 2-propanol after 24 h. The crystals belonged to orthorhombic space group $P2_12_12$ with the following unit cell dimensions: $a = 64.3$ Å, $b = 91.3$ Å, and $c = 118.9$ Å.

Data Collection and Structure Solution. Data were collected at the European Synchrotron Radiation Facility (ESRF), beamline ID14-2, using an ADSC CCD detector and a wavelength of 0.933 Å with a crystal-to-detector distance of 130 mm. All diffraction data were processed with Denzo and scaled with Scalepack (*29*). The asymmetric unit contained two heterodimeric molecules (Table 1). The structure was determined by molecular replacement using AmoRe (*30*) implemented in the Collaborative Computational Project Number 4 (CCP4) suite of programs. The α-chain of botrocetin [PDB entry 1FVU (*10*)] was used as a search model. For the rotation and translation searches, data in the range of 7−2 Å were used. A total number of four solutions were found which were inspected graphically. The correlation coefficient of the solutions was 51.9 and the R_{factor} 56.6. The phases were significantly improved by performing noncrystallographic symmetry using the density modification package (DM). This resulted in the production of a high-quality electron density map allowing construction of the aggretin model.

Refinement. All crystallographic refinements were carried out using REFMAC 5 (*31*). Several cycles of model building and refinement caused R_{factor} and R_{free} to drop below 30%.

Table 1: Summary of Crystallographic Analysis[a]

space group	$P2_12_12$
unit cell dimensions	64.3 Å, 91.3 Å, 118.9 Å, 90°, 90°, 90°
resolution range (Å)	40.0−1.7
no. of unique reflections	93101
completeness (%)	99.9 (100)
$I/\sigma(I)$	42.55 (2.59)
R_{merge}	0.056 (0.460)
redundancy	4.3
no. of reflections for refinement	87812
final R_{free} (%)	23.6
final R (%)	20.2
rmsd for bonds (Å)	0.20
rmsd for angles (deg)	1.876
mean B value for the main chain (Å^2)	22.31
mean B value for the side chain (Å^2)	24.33
mean B value for the whole chain (Å^2)	23.35
mean B value for water (Å^2)	32.56
Ramachandran plot	
most favored and additional regions	99.8%
generous and disallowed regions	0.2% (one residue, Lys60)

[a] $R_{merge} = \sum|I - \langle I\rangle|\sum I$, where I is the observed intensity and $\langle I\rangle$ is the average intensity of multiple observations of symmetry-related reflections. $R = \sum||F_o| - |F_c||/\sum|F_o|$. R_{free} is calculated for a randomly selected 5% of the reflections. R_{factor} is calculated for the remaining 95% of the reflections used in refinement.

Water molecules were then located using ArpWarp (*32*), and two sulfate molecules were also added. Further refinement cycles yielded an R_{factor} of 20.2% and an R_{free} of 23.6%. The final model of a single aggretin heterodimer is comprised of two α- and β-subunits. The α-chain contains 132 amino acids and the β-chain 121. In total, six amino acids could not be identified, all of which are part of the termini of the two chains. The stereochemistry of the final model was validated using Procheck (*33*).

Analysis of the Interaction of Aggretin with Platelet Surface Receptor CLEC-2 by Docking. Crystal structures of CLEC-2 (PDB entry 2C6U) and aggretin were prepared for docking with WHATIF (*34*). Patchdock (*35*) was used for docking calculations for the interaction of aggretin and CLEC-2. Site-directed mutagenesis studies of CLEC-2 have indicated that electrostatic interactions are involved in its interaction with aggretin, and these were taken into consideration while calculating the docking interaction (*21*). A molecular shape representation was performed by computing the molecular surface of the molecule. This was followed by a segmentation algorithm which detected geometric patches; these were filtered, and then a geometric hashing and pose-clustering matching was performed to match the patches on two structures. The top 10 solutions from each round of calculations were manually checked for interaction sites and orientation of the molecules. Models were subjected to a 500 ps refinement followed by energy minimization.

Molecular Dynamics Simulation for Refinement of Docked Structures. The MD simulations were performed using YASARA dynamics (*34*). A simulation cell was constructed around the docked structures with a 7.9 Å cutoff for the electrostatic forces, which were calculated using the particle mesh Ewald method. The pK_a values of the ionizable groups in the docked structure were predicted and assigned the protonation states based on pH 7.2. The cell was filled with water, and the AMBER99 (*35*) electrostatic potential was evaluated at all water molecules; the one with the lowest or highest potential was turned into a sodium or chloride

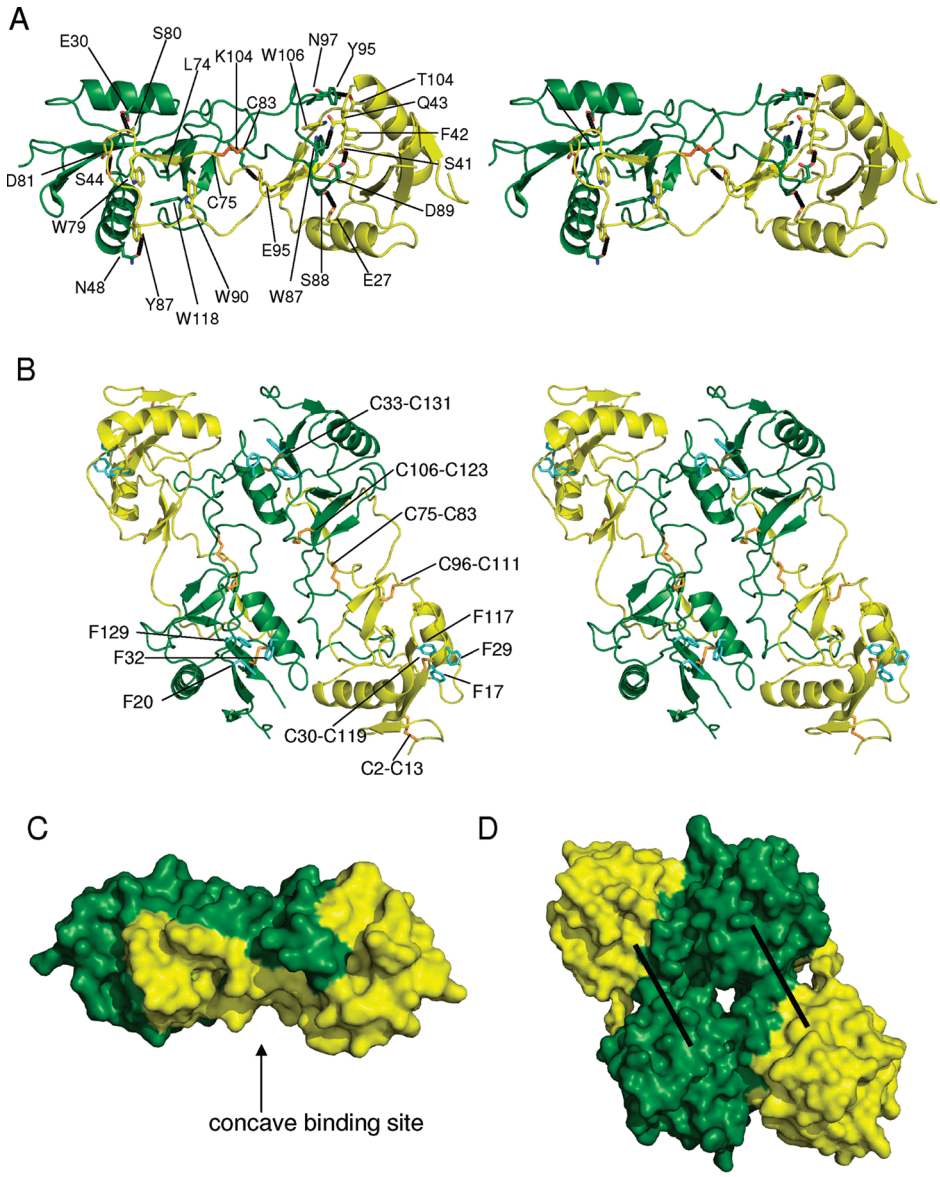

FIGURE 1: (A) Stereoview of the topology of the structure of the aggretin $\alpha\beta$-heterodimer. The α-subunit is colored green and the β-subunit yellow. Residues that form hydrogen bonds or hydrophobic interactions across the dimer interface are highlighted. Hydrogen bonds between side chains are shown as black dashed lines. (B) Stereoview of the topology of the quaternary structure of $(\alpha\beta)_2$ aggretin. The disulfide bonds of the $\alpha\beta$-heterodimer are colored orange. The phenylalanine residues which form a π-stacking network in the globular domains are colored cyan. (C) Surface representation of the side view of $(\alpha\beta)_2$ aggretin (same orientation as in panel A). (D) Surface representation of $(\alpha\beta)_2$ aggretin (same orientation as in panel B). The concave receptor binding site is shown with a black line.

counterion until the cell was neutral. A short steepest descent minimization of all atoms removed severe bumps followed by simulated annealing minimizations at 298 K. Velocities were scaled down every 10 steps for a total time of 5 ps in 500 steps. A start-up simulation was then run for 5 ps, using a multiple time step of 1 fs for intramolecular and 2 fs for intermolecular forces, with all heavy protein atoms fixed, so that the solvent molecules could smoothly cover the protein surface. Simulated annealing minimizations were started at 298 K, and velocities were scaled down every 10 steps for a total time of 5 ps in 500 steps. Molecular dynamics simulations were run with the AMBER99 force field at 298 K and 0.9% NaCl in the simulation cell for 500 ps to refine the docked structures.

RESULTS

Aggretin Structure. Aggretin, like other members of the C-type lectin-like family, is composed of two structurally homologous subunits, α and β, that form a disulfide-linked heterodimer with each subunit containing a compact lectin-like globular domain and a long extended loop region (Figure 1A). Superposition of the α- and β-subunits gives a rmsd of 1.7 Å. The α- and β-subunits of aggretin have a low degree of sequence homology of 38%, and the globular domains have a predominantly hydrophobic core, which includes a perpendicular π-stacking network between the Phe20-Phe32-Phe129 motif in subunit α and the Phe17-Phe29-Phe117 motif in subunit β (Figure 1B). The α-subunit has two disulfide bonds (Cys33−Cys131 and Cys106−Cys123), whereas the β-subunit has three disulfide bonds (Cys2−Cys13, Cys30−Cys119, and Cys96−Cys111) which are conserved in other members of the C-type lectin-like family of snake venom proteins (Figure 1B). Aggretin is highly homologous in sequence (~50%) and structure with other members of the C-type lectin-like protein superfamily (Figure 2B and Figure S1 of the Supporting Information). These all [botro-

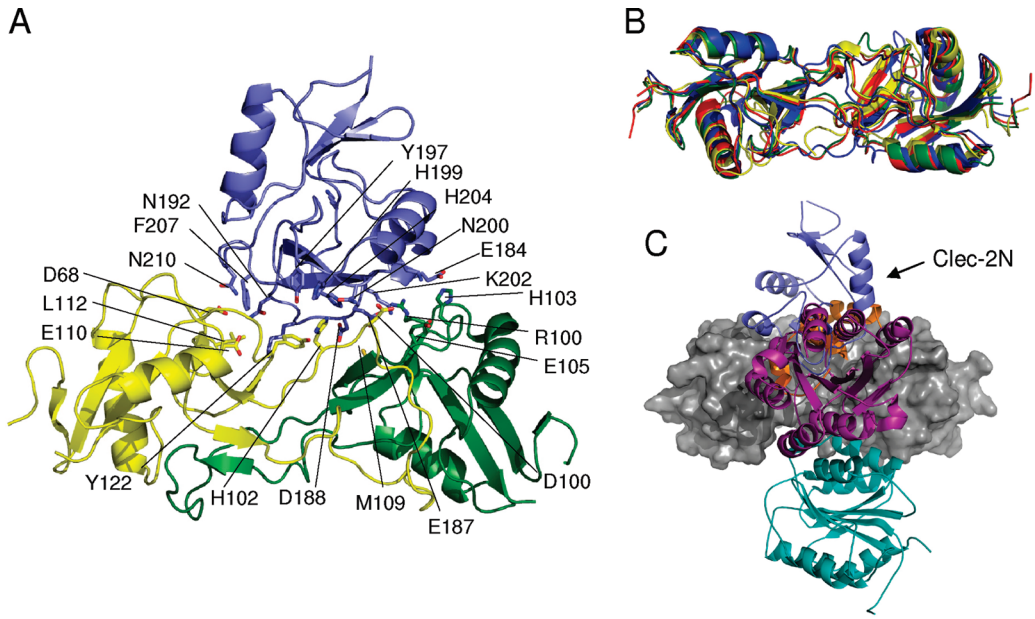

FIGURE 2: (A) Model of CLEC-2N docked with an aggretin $\alpha\beta$-heterodimer. Residues involved in the interaction between CLEC-2N and aggretin are highlighted in stick format. CLEC-2 is colored blue, the aggretin α-subunit green, and the aggretin β-subunit yellow. (B) Superposition of the $\alpha\beta$-heterodimers of the structurally homologous C-type lectin-like snake venom proteins aggretin (green), EMS16 (blue), botrocetin (yellow), and flavocetin (red). (C) Diagram showing the positions of binding of different ligands to C-type lectin-like snake venom proteins depicted in panel B: CLEC-2 (blue), the Gla domain of factor IX (orange), the integrin α2-I domain (purple), and the A1 domain of von Willebrand factor (turquoise). These ligands bind aggretin (gray), IX-bp, EMS16, and botrocetin, respectively.

cetin (*10*), IX/X-bp (*7*), convulxin (*5*), flavocetin (*8*), echicetin (*6*), and aggretin] form $\alpha\beta$-heterodimers through domain swapping of the extended loop region, and complex crystal structures have revealed that ligand binding usually occurs in a centrally located concave surface involving contacts with the extended loops.

The quaternary structure of aggretin is a novel $(\alpha\beta)_2$ tetramer which forms into an antiparallel structure due to a 2-fold rotation (Figure 1B). The interface buried upon formation of the tetramer has a large surface area (11710 Å^2, 35% of the total surface area), and it remains a tetramer in gel filtration experiments (*14*). The side-by-side arrangement causes the concave surface of the $\alpha\beta$-heterodimer saddle shape to be oriented on the same face (Figure 1C,D). Interactions between the two dimers are primarily between the α-subunits with helix α1 interacting with the opposing α-chain extended loop. There are main chain−side chain interactions between Glu28 and Ile99, Lys31 and Leu101, Lys31 and Leu98, and Arg34 and Ser94 and side chain−side chain interactions between Arg43 and Glu80. The majority of these side chains are not conserved in other C-type lectin-like snake venom proteins, including purpureotin and aglucetin which have both been shown to be tetrameric (Figure 1B). The crystal structures have yet to be determined for these proteins although, purpureotin has been modeled as a parallel dimer (*36, 37*).

Several snake venom C-type lectin-like proteins have divalent cation binding sites within their globular domains. Factor IX/X-binding protein (FIX/X-bp) has Ca^{2+} binding sites in both α- and β-subunits (*7*); botrocetin has one Ca^{2+} binding site, its β-subunit, but convulxin, flavocetin, and aggretin lack divalent cation binding sites (*5, 8, 10*). Assays of aggretin activity in the presence of EDTA suggested that its function was independent of divalent cations, and the aggretin structure reveals no bound cations (*14*). The cation binding site in the α-subunit of FIX/X-bp consists of Ser41, Glu43, Glu47, and Glu128 and in the β-subunit Ser41, Glu43, Glu47, and Glu122 which forms a negatively charged cation binding pocket in IX/X-bp. In aggretin, only homologous residues Ser44, Glu46, and Glu50 are conserved in both α- and β-subunits whereas Glu128 and Glu122 of IX/X-bp are replaced with Lys132 and Lys120, respectively. These latter substitutions alter the charge of the pocket, and the terminal nitrogen atom of the lysine residues stabilizes both pockets in the absence of divalent cation.

Docking of Aggretin and the CLEC-2 N-Terminal Domain. Aggretin is thought to activate platelets by binding and clustering receptor CLEC-2. The interaction between aggretin and the recombinant N-terminal domain of CLEC-2 (CLEC-2N) has been shown to have a dissociation constant of 1 μM (*21*). To investigate the basis of this interaction, we performed molecular docking with the aggretin $\alpha\beta$-heterodimer and the CLEC-2N crystal structure (*21*). Patchdock (*35*) was used for molecular docking calculations, and the complex with the best fit to the available biochemical data was selected from the top three scoring structures. In this complex, the CLEC-2N domain is positioned covering the concave surface between the aggretin $\alpha\beta$-lectin-like domains and is slightly off center positioned closer to the β-subunit than α. Principal contacts are formed between CLEC-2N and both the α- and β-subunit lectin-like domains and long loops with a series of salt bridges defining the key interactions (Figure 2A). From the interface, a short helix from CLEC-2N contributes residue Glu184 which contacts the aggretin β-subunit His103; interactions extend from here along the semihelical long loop region, including CLEC-2N Glu187 forming a salt bridge with β-subunit Arg100, and at the opposing end, CLEC-2N Lys190 interacts with the α-subunit side chain Glu110. Further contacts with the aggretin α-subunit are made through CLEC-2N Phe207 and Asn210 contacting Leu112 and Asp68, respectively, and at the opposite end of the CLEC-2 sheet, residues Asn200 and

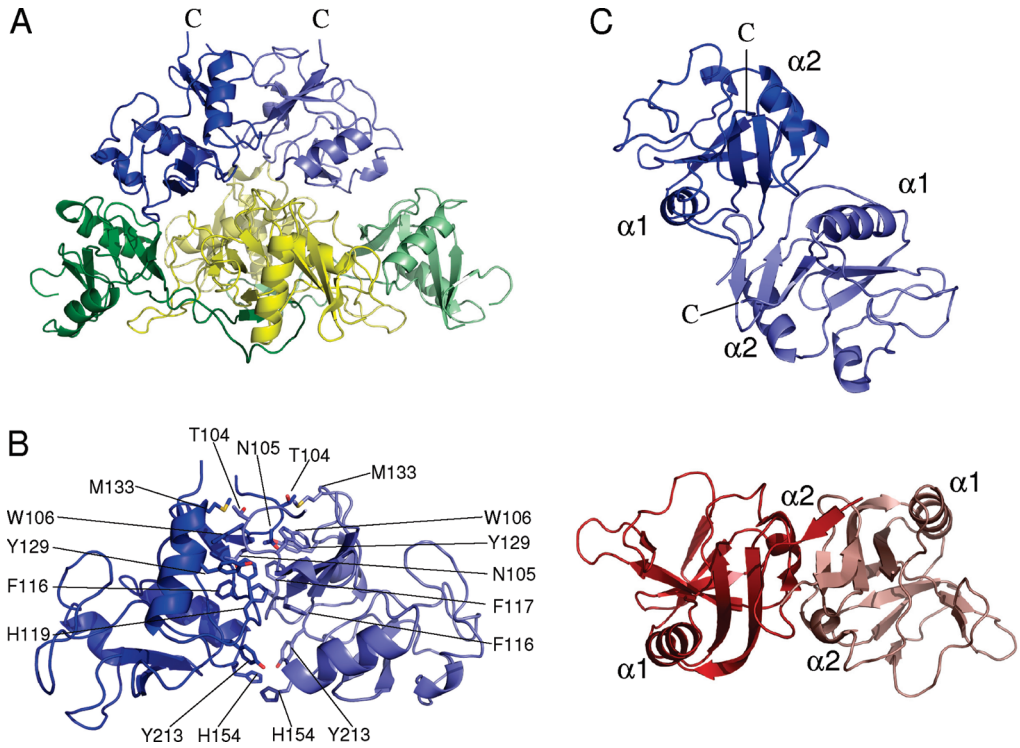

FIGURE 3: (A) CLEC-2N−aggretin complex superimposed onto the aggretin $(\alpha\beta)_2$ tetramer. CLEC-2N is colored blue, the aggretin α-subunit green, and the aggretin β-subunit yellow. The $\alpha\beta$-heterodimers and two CLEC-2N molecules are differentiated by darker and lighter shading. The N- and C-termini are labeled. (B) Dimer interface of CLEC-2N as determined by superimposing the CLEC-2N−aggretin complex onto the aggretin tetramer. The interface is predominantly hydrophobic, and those residues involved in dimer formation are highlighted. (C) Comparison of the CLEC-2N (blue) dimer of the CLEC-2N−aggretin complex and the structure of immune receptor NGK2D (red) of the NKG2D−ULBP3 complex (PDB entry 1KCG). The left-hand monomer of each dimer is in the same orientation, thus showing the 45° rotation of the domains.

Lys202 pack against Asp100 from the α-subunit and Glu105 from the β-subunit.

Mutagenic studies of CLEC-2N implicate the long loop, and more specifically residues Lys150, Lys171, Glu184, Asp188, Lys190, and Asn192, as being involved in aggretin binding, and this is in broad agreement with the model (*21*). One discrepancy is that CLEC-2N residue Asp188 is predicted to contribute to binding, but in the model, this only makes an incidental contact with Met109 from the β-subunit. The CLEC-2N and aggretin structures are essentially treated as rigid bodies in this docking experiment, and one area of the structure which can potentially undergo conformational change upon formation of the complex is the CLEC-2N long loop (*21*). This could undergo a change in conformation to form a better fit into the aggretin groove, and as a result, Asp188 may form more direct interactions. In addition to the residues previously identified, the model of CLEC-2N docked with aggretin also predicts that Asn210, His199, Lys202, and His204 may be important in CLEC-2−aggretin binding.

The model of the aggretin−CLEC-2N complex is similar to the ligand complex crystal structures of snake venom C-type lectins. Figure 2C shows structures for the EMS16−integrin α2-I domain, botrocetin−von Willebrand factor A1 domain, and factor IX binding protein−factor IX Gla domain complexes superposed onto the aggretin−/CLEC-2N model, and the alignment of the sequences illustrates the overlap in the binding footprint (Figure S1 of the Supporting Information). Differences between the mode of action exist as both EMS16 and factor IX binding protein have a function blocking role and structurally exist as $\alpha\beta$-dimers, whereas aggretin activates platelets and has the $(\alpha\beta)_2$ structure with a clustering function.

Dimerization of CLEC-2N by Aggretin. Dimerization of CLEC-2 would be an expected consequence of aggretin binding as it is thought to activate platelets by clustering the receptor, thus bringing the cytoplasmic domains closer together, enabling efficient phosphorylation of the YXXL motif (*24, 38*). Figure 3A illustrates the CLEC-2N−aggretin complex superposed onto the aggretin tetramer. Here the two CLEC-2N domains are brought into proximity and "fit together" forming a small interface, effectively bringing the N- and C-termini together through contact of residues 101−133 (two β-strands, helix α1, and loop regions). Hydrophobic contacts are formed by Phe117 side chains at the center of the interface close to the 2-fold axis with further side chain−main chain contacts occurring on either side, with the His119 NE2 atom forming a hydrogen bond to the Asn105 carbonyl oxygen and the Tyr129 OH group forming a hydrogen bond to the main chain nitrogen of Trp106. Above this, as depicted in Figure 3B, the side chain from Thr104 packs against Met133 and Asn105 packs against Trp106. Below this, Tyr213 hydrogen bonds to the main chain nitrogen of His154 from helix α1.

Further evidence to support the CLEC-2N−aggretin model of CLEC-2 dimerization comes from the structurally homologous lectin-like proteins with immune functions, such as receptors NKG2D, LOX-1, and Ly49C (*39–41*). Here crystal structures are available for dimers of both unliganded and ligand complexed crystal structures, and in the case of NKG2D, the structure of the dimer is remarkably similar to that of CLEC-2N. The difference is shown in Figure 3C as

a 45° rotation of the domains such that instead of the helix α2 forming contacts on the 2-fold axis it is the adjacent β-sheet which interlocks. We next examined whether the CLEC-2N domain could form a dimer structure similar to the immune receptors by superposing the CLEC-2N structure onto the dimer structures of NKG2D, LOX-1, and Ly49C, and in each case, there were steric clashes indicating these dimerization modes are unlikely for CLEC-2N.

DISCUSSION

The structure of aggretin reveals a novel tetrameric $(\alpha\beta)_2$ quaternary structure in which aggretin presents two adjacent receptor binding sites supporting a receptor clustering mechanism of action. This is similar to the clustering of GPVI and GPIbα by convulxin and flavocetin A, respectively. The αβ-heterodimers of convulxin and flavocetin A are structurally homologous to that of aggretin; however, their quaternary structure is quite different. Convulxin and flavocetin A are both disulfide-linked cyclic tetramers of $(\alpha\beta)_4$ structure with the disulfide bond between the C-terminus of the α-subunit and the N-terminus of the β-subunit (*8, 42*). This allows for the binding and clustering of four ligand (GPVI) molecules. Aggretin on the other hand has no free cysteine residues and therefore cannot form a cyclic structure similar to convulxin and flavocetin A and instead forms a noncovalent $(\alpha\beta)_2$ dimer. A series of reports suggest that CLEC-2 is the principal platelet receptor ligand for aggretin but that GPIbα and α2β1 may have supplementary roles in the same way as in other snake venom C-type lectin-like proteins (*12*). Podoplanin, which is involved in pathological tumor cell-induced platelet aggregation, has also been shown to bind CLEC-2 (*23, 24*). The interaction of podoplanin with CLEC-2 results in a signaling response, which subsequently leads to platelet aggregation, similar to that induced by aggretin−CLEC-2 binding. In spite of this similarity, it appears that aggretin and podoplanin interact with CLEC-2 in a different manner. The interaction of aggretin and CLEC-2 is restricted to the concave surface of aggretin and the C-terminal loop of CLEC-2. This interaction mainly involves hydrogen bonds between the side chains of the two proteins and has been identified by mutagenic studies. The structure of aggretin shows that there are no glycosylation sites, or other post-translational modifications, which could be involved in CLEC-2 binding. The binding site for CLEC-2 in podoplanin has been shown to involve the sialic acid group of *O*-glycan on Thr52 and residues 38−54 which surround it. Podoplanin has been shown to bind to an area which is predominantly positively charged on the surface of CLEC-2N (residues 87−147) (*24*). Sialic acid has several hydroxyl groups, all of which are potential hydrogen bond donors, and sialic acid also causes a slight negative charge on the surface of the protein. These data show that aggretin and podoplanin have different binding sites on CLEC-2, suggesting that it is the clustering of the ligand which determines the downstream effects, not the isolated binding of a ligand to the extracellular domain (*24*).

In the absence of a high-resolution complex crystal structure, the aggretin−CLEC-2N model provides predictions which can be tested through functional analysis and contributes to our understanding of platelet activation and aggregation and may also help further improve our understanding of the basis of the "platelet cloak" which contributes to tumor cell survival and metastasis mediated by receptor podoplanin.

ACKNOWLEDGMENT

We thank the staff at the European Synchrotron Research Facility beamline ID 14-2 for their assistance with data collection and David Leys for his advice on molecular replacement calculations.

SUPPORTING INFORMATION AVAILABLE

Sequence alignment of the α- and β-chains of aggretin, IX-bp, EMS16, and botrocetin showing conserved residues and residues involved in ligand binding (Figure S1). This material is available free of charge via the Internet at http://pubs.acs.org.

REFERENCES

1. Andrews, R. K., and Berndt, M. C. (2000) Snake venom modulators of platelet adhesion receptors and their ligands. *Toxicon 38*, 775–791.
2. Morita, T. (2005) Structures and functions of snake venom CLPs (C-type lectin-like proteins) with anticoagulant-, procoagulant-, and platelet-modulating activities. *Toxicon 45*, 1099–1114.
3. Matsui, T., and Hamako, J. (2005) Structure and function of snake venom toxins interacting with human von Willebrand factor. *Toxicon 45*, 1075–1087.
4. Braud, S., Bon, C., and Wisner, A. (2000) Snake venom proteins acting on hemostasis. *Biochimie 82*, 851–859.
5. Batuwangala, T., Leduc, M., Gibbins, J. M., Bon, C., and Jones, E. Y. (2004) Structure of the snake-venom toxin convulxin. *Acta Crystallogr. D60*, 46–53.
6. Jasti, J., Paramasivam, M., Srinivasan, A., and Singh, T. P. (2004) Crystal structure of echicetin from *Echis carinatus* (Indian saw-scaled viper) at 2.4 Å resolution. *J. Mol. Biol. 335*, 167–176.
7. Mizuno, H., Fujimoto, Z., Koizumi, M., Kano, H., Atoda, H., and Morita, T. (1997) Structure of coagulation factors IX/X-binding protein, a heterodimer of C-type lectin domains. *Nat. Struct. Biol. 4*, 438–441.
8. Fukuda, K., Mizuno, H., Atoda, H., and Morita, T. (2000) Crystal structure of flavocetin-A, a platelet glycoprotein Ib-binding protein, reveals a novel cyclic tetramer of C-type lectin-like heterodimers. *Biochemistry 39*, 1915–1923.
9. Hirotsu, S., Mizuno, H., Fukuda, K., Qi, M. C., Matsui, T., Hamako, J., Morita, T., and Titani, K. (2001) Crystal structure of bitiscetin, a von Willebrand factor-dependent platelet aggregation inducer. *Biochemistry 40*, 13592–13597.
10. Sen, U., Vasudevan, S., Subbarao, G., McClintock, R. A., Celikel, R., Ruggeri, Z. M., and Varughese, K. I. (2001) Crystal structure of the von Willebrand factor modulator botrocetin. *Biochemistry 40*, 345–352.
11. Huang, T. F., Liu, C. Z., and Yang, S. H. (1995) Aggretin, a novel platelet-aggregation inducer from snake (*Calloselasma rhodostoma*) venom, activates phospholipase C by acting as a glycoprotein Ia/IIa agonist. *Biochem. J. 309* (Part 3), 1021–1027.
12. Shin, Y., and Morita, T. (1998) Rhodocytin, a functional novel platelet agonist belonging to the heterodimeric C-type lectin family, induces platelet aggregation independently of glycoprotein Ib. *Biochem. Biophys. Res. Commun. 245*, 741–745.
13. Chung, C. H., Au, L. C., and Huang, T. F. (1999) Molecular cloning and sequence analysis of aggretin, a collagen-like platelet aggregation inducer. *Biochem. Biophys. Res. Commun. 263*, 723–727.
14. Navdaev, A., Clemetson, J. M., Polgar, J., Kehrel, B. E., Glauner, M., Magnenat, E., Wells, T. N., and Clemetson, K. J. (2001) Aggretin, a heterodimeric C-type lectin from *Calloselasma rhodostoma* (malayan pit viper), stimulates platelets by binding to α2β1 integrin and glycoprotein Ib, activating Syk and phospholipase Cγ2, but does not involve the glycoprotein VI/Fc receptor γ chain collagen receptor. *J. Biol. Chem. 276*, 20882–20889.

15. Shiraishi, M., Ogawa, H., Ikeda, M., Kawashima, S., and Ito, K. (2002) Platelet dysfunction in Chediak-Higashi syndrome-affected cattle. *J. Vet. Med. Sci. 64*, 751–760.
16. Chung, C. H., Peng, H. C., and Huang, T. F. (2001) Aggretin, a C-type lectin protein, induces platelet aggregation via integrin $\alpha_2\beta_1$ and GPIb in a phosphatidylinositol 3-kinase independent pathway. *Biochem. Biophys. Res. Commun. 285*, 689–695.
17. Bergmeier, W., Bouvard, D., Eble, J. A., Mokhtari-Nejad, R., Schulte, V., Zirngibl, H., Brakebusch, C., Fassler, R., and Nieswandt, B. (2001) Rhodocytin (aggretin) activates platelets lacking $\alpha_2\beta_1$ integrin, glycoprotein VI, and the ligand-binding domain of glycoprotein Ibα. *J. Biol. Chem. 276*, 25121–25126.
18. Suzuki-Inoue, K., Ozaki, Y., Kainoh, M., Shin, Y., Wu, Y., Yatomi, Y., Ohmori, T., Tanaka, T., Satoh, K., and Morita, T. (2001) Rhodocytin induces platelet aggregation by interacting with glycoprotein Ia/IIa (GPIa/IIa, Integrin $\alpha2\beta1$). Involvement of GPIa/IIa-associated src and protein tyrosine phosphorylation. *J. Biol. Chem. 276*, 1643–1652.
19. Eble, J. A., Beermann, B., Hinz, H. J., and Schmidt-Hederich, A. (2001) $\alpha2\beta1$ integrin is not recognized by rhodocytin but is the specific, high affinity target of rhodocetin, an RGD-independent disintegrin and potent inhibitor of cell adhesion to collagen. *J. Biol. Chem. 276*, 12274–12284.
20. Suzuki-Inoue, K., Fuller, G. L., Garcia, A., Eble, J. A., Pohlmann, S., Inoue, O., Gartner, T. K., Hughan, S. C., Pearce, A. C., Laing, G. D., Theakston, R. D., Schweighoffer, E., Zitzmann, N., Morita, T., Tybulewicz, V. L., Ozaki, Y., and Watson, S. P. (2006) A novel Syk-dependent mechanism of platelet activation by the C-type lectin receptor CLEC-2. *Blood 107*, 542–549.
21. Watson, A. A., Brown, J., Harlos, K., Eble, J. A., Walter, T. S., and O'Callaghan, C. A. (2007) The crystal structure and mutational binding analysis of the extracellular domain of the platelet-activating receptor CLEC-2. *J. Biol. Chem. 282*, 3165–3172.
22. Chaipan, C., Soilleux, E. J., Simpson, P., Hofmann, H., Gramberg, T., Marzi, A., Geier, M., Stewart, E. A., Eisemann, J., Steinkasserer, A., Suzuki-Inoue, K., Fuller, G. L., Pearce, A. C., Watson, S. P., Hoxie, J. A., Baribaud, F., and Pohlmann, S. (2006) DC-SIGN and CLEC-2 mediate human immunodeficiency virus type 1 capture by platelets. *J. Virol. 80*, 8951–8960.
23. Suzuki-Inoue, K., Kato, Y., Inoue, O., Kaneko, M. K., Mishima, K., Yatomi, Y., Yamazaki, Y., Narimatsu, H., and Ozaki, Y. (2007) Involvement of the snake toxin receptor CLEC-2, in podoplanin-mediated platelet activation, by cancer cells. *J. Biol. Chem. 282*, 25993–26001.
24. Kato, Y., Kaneko, M. K., Kunita, A., Ito, H., Kameyama, A., Ogasawara, S., Matsuura, N., Hasegawa, Y., Suzuki-Inoue, K., Inoue, O., Ozaki, Y., and Narimatsu, H. (2008) Molecular analysis of the pathophysiological binding of the platelet aggregation-inducing factor podoplanin to the C-type lectin-like receptor CLEC-2. *Cancer Sci. 99*, 54–61.
25. Wicki, A., Lehembre, F., Wick, N., Hantusch, B., Kerjaschki, D., and Christofori, G. (2006) Tumor invasion in the absence of epithelial-mesenchymal transition: Podoplanin-mediated remodeling of the actin cytoskeleton. *Cancer Cell 9*, 261–272.
26. Mishima, K., Kato, Y., Kaneko, M. K., Nakazawa, Y., Kunita, A., Fujita, N., Tsuruo, T., Nishikawa, R., Hirose, T., and Matsutani, M. (2006) Podoplanin expression in primary central nervous system germ cell tumors: a useful histological marker for the diagnosis of germinoma. *Acta Neuropathol. 111*, 563–568.
27. Kato, Y., Sasagawa, I., Kaneko, M., Osawa, M., Fujita, N., and Tsuruo, T. (2004) Aggrus: A diagnostic marker that distinguishes seminoma from embryonal carcinoma in testicular germ cell tumors. *Oncogene 23*, 8552–8556.
28. Kaneko, M. K., Kato, Y., Kameyama, A., Ito, H., Kuno, A., Hirabayashi, J., Kubota, T., Amano, K., Chiba, Y., Hasegawa, Y., Sasagawa, I., Mishima, K., and Narimatsu, H. (2007) Functional glycosylation of human podoplanin: Glycan structure of platelet aggregation-inducing factor. *FEBS Lett. 581*, 331–336.
29. Otwinowski, Z., and Minor, W. (1997) Processing of X-ray diffraction data collected in oscillation mode. *Methods Enzymol. 276*, 307–326.
30. Navaza, J. (1994) AMoRE: An automated package for molecular replacement. *Acta Crystallogr. A50*, 157–163.
31. Murshudov, G., Vagin, A., and Dodson, E. (1997) Refinement of Macromolecular Structures by the Maximum-Likelihood Method. *Acta Crystallogr. D53*, 240–255.
32. Perrakis, A., Morris, R. M., and Lamzin, V. S. (1999) Automated protein model building combined with iterative structure refinement. *Nat. Struct. Biol. 6*, 458–463.
33. Laskowski, R. A., Moss, D. S., and Thornton, J. M. (1993) Main-chain bond lengths and bond angles in protein structures. *J. Mol. Biol. 231*, 1049–1067.
34. Krieger, E., Darden, T., Nabuurs, S. B., Finkelstein, A., and Vriend, G. (2004) Making optimal use of empirical energy functions: Force-field parameterization in crystal space. *Proteins 57*, 678–683.
35. Liu, H., Elstner, M., Kaxiras, E., Frauenheim, T., Hermans, J., and Yang, W. (2001) Quantum mechanics simulation of protein dynamics on long timescale. *Proteins 44*, 484–489.
36. Li, X., Zheng, L., Kong, C., Kolatkar, P. R., and Chung, M. C. (2004) Purpureotin: A novel di-dimeric C-type lectin-like protein from *Trimeresurus purpureomaculatus* venom is stabilized by noncovalent interactions. *Arch. Biochem. Biophys. 424*, 53–62.
37. Wang, W. J., and Huang, T. F. (2001) A novel tetrameric venom protein, agglucetin from *Agkistrodon acutus*, acts as a glycoprotein Ib agonist. *Thromb. Haemostasis 86*, 1077–1086.
38. Fuller, G. L., Williams, J. A., Tomlinson, M. G., Eble, J. A., Hanna, S. L., Pohlmann, S., Suzuki-Inoue, K., Ozaki, Y., Watson, S. P., and Pearce, A. C. (2007) The C-type lectin receptors CLEC-2 and Dectin-1, but not DC-SIGN, signal via a novel YXXL-dependent signaling cascade. *J. Biol. Chem. 282*, 12397–12409.
39. Radaev, S., Rostro, B., Brooks, A. G., Colonna, M., and Sun, P. D. (2001) Conformational plasticity revealed by the cocrystal structure of NKG2D and its class I MHC-like ligand ULBP3. *Immunity 15*, 1039–1049.
40. Ohki, I., Ishigaki, T., Oyama, T., Matsunaga, S., Xie, Q., Ohnishi-Kameyama, M., Murata, T., Tsuchiya, D., Machida, S., Morikawa, K., and Tate, S. (2005) Crystal structure of human lectin-like, oxidized low-density lipoprotein receptor 1 ligand binding domain and its ligand recognition mode to OxLDL. *Structure 13*, 905–917.
41. Dam, J., Guan, R., Natarajan, K., Dimasi, N., Chlewicki, L. K., Kranz, D. M., Schuck, P., Margulies, D. H., and Mariuzza, R. A. (2003) Variable MHC class I engagement by Ly49 natural killer cell receptors demonstrated by the crystal structure of Ly49C bound to H-2K(b). *Nat. Immunol. 4*, 1213–1222.
42. Murakami, M. T., Zela, S. P., Gava, L. M., Michelan-Duarte, S., Cintra, A. C., and Arni, R. K. (2003) Crystal structure of the platelet activator convulxin, a disulfide-linked $\alpha4\beta4$ cyclic tetramer from the venom of *Crotalus durissus terrificus*. *Biochem. Biophys. Res. Commun. 310*, 478–482.

BI800528T